TRENDS IN SCIENCES 2026; 23(2): 11629
https://doi.org/10.48048/tis.2026.11629 RESEARCH ARTICLE

Approach Towards Sustainable Synthesis of Silver Nanoparticles by Electrolysis Method Using Asian Pennywort Extract and Their Anti-Inflammatory Activity

Dhony Hermanto[1,*], Nurul Ismillayli[1] and Rahadi Wirawan[2]

[1]Department of Chemistry, Faculty of Mathematics and Natural Sciences, University of Mataram, Mataram, West Nusa Tenggara 83125, Indonesia
[2]Department of Physics, Faculty of Mathematics and Natural Sciences, University of Mataram, Mataram, West Nusa Tenggara 83125, Indonesia

([*]Corresponding author's e-mail: dhony.hermanto@unram.ac.id)

Received: 18 August 2025, Revised: 4 September 2025, Accepted: 14 September 2025, Published: 30 November 2025

Abstract

Biogenic metal nanoparticles continue gaining popularity due to their low production costs, biocompatibility, and several environmental and biological benefits. In this work, Asian pennywort extract (APE) will be electrolysed to produce biogenic silver nanoparticles (AgNPs) sustainably. This study also aims to improve APE's in vitro anti-inflammatory properties. The extract solution acts as an electrolyte in the system, facilitating the formation of AgNPs via electrochemical synthesis, as shown by the appearance of a peak at 430 nm. In accordance with the FTIR spectra, the phytochemical screening findings of the extract showed a preponderance of phenols, flavonoids, and triterpenes. It suggests that the biomolecules in the extract serve as both stabilising and reducing agents, playing a role in the synthesis process. TEM micrographs demonstrate that AgNPs have a uniform spherical shape and are surrounded by a thin biomolecular layer with diameters of 32.62 ± 10.53 nm. The light scattering pattern of colloidal AgNPs also exhibits a particle size distribution of 32.50 ± 5.68 nm. The approach generates polycrystalline nanoparticles ranging in size from 17.55 to 32.26 nm. AgNPs outperformed APE in terms of anti-inflammatory action, with IC_{50} values of 523.40 ± 7.85 and 960.29 ± 16.81 µg/mL, as determined by the BSA protein denaturation procedure. The electrosynthesis approach using APE biomolecules suggests a novel strategy for producing AgNPs with superior anti-inflammatory capabilities, leading to promising future applications for large-scale production in the pharmaceutical and cosmetics industries.

Keywords: Silver nanoparticle, Electrolysis method, Asian pennywort extract, Anti-inflammatory activity

Introduction

Anti-inflammatory drugs are medicines used to reduce inflammation in the body. Inflammation is the body's natural response to injury or infection; however, excessive inflammation can cause pain and discomfort. Nonsteroidal anti-inflammatory drugs (NSAIDs), which are most commonly used to decrease inflammation, relieve pain, and lower fever, work by blocking the production of chemicals in the body that trigger inflammation [1]. However, these drugs often have side effects such as stomach ulcers, bleeding, and kidney problems [2]. Therefore, medicinal plants are a common source of active chemicals with fewer side effects [3,4]. Because the active compounds are present in low concentrations, the therapeutic effects of medicinal plants might not be immediately noticeable [5]. It takes time for these compounds to accumulate in the body to reach effective levels. This has led to research into fast-acting anti-inflammatories with fewer side effects.

Red Blood Cell (HRBC) membrane stabilisation and heat-induced haemolysis assay, where AgNPs prepared using the polyol method showed a maximum inhibition of 73.6%, compared to 84.8% for the reference standard, diclofenac sodium [6]. Chi *et al.* [7] conducted a study demonstrating that the anti-inflammatory activity of AgNPs synthesised using aqueous Azadirachta indica kernel extract was

comparable to that of the standard drug when administered at a concentration of 100 µg/mL. Additionally, Varghese *et al.* [8] investigated AgNPs and zinc oxide synthesised using Ocimum tenuiflorum and Ocimum gratissimum and observed potent anti-inflammatory activity that matched that of diclofenac sodium, a standard anti-inflammatory drug; thus, these findings further support the potential of AgNPs as an effective agent for managing inflammation. It is estimated that AgNP products will continue to increase, driving demand due to their unique qualities (chemical stability, size, shape, homogeneity, and catalytic activity) [9]. This development is pursued in nanotechnology schemes, such as designing biogenic AgNPs with excellent characteristics and coating agents that can enhance anti-inflammatory action.

The preparation of AgNPs and their various applications has been one of the primary focuses of nanotechnology research. Although various physical and chemical methods for synthesising AgNPs have been described, the majority are expensive or use hazardous compounds, which are undesirable due to their detrimental health and environmental impacts. Biogenic AgNP synthesis has grown simpler, less expensive, and more efficient as a result of the use of numerous green chemistry principles [10-12]. Biogenic AgNPs were created utilising green tea leaves extract, which has good antioxidant [13] and antibacterial [14] characteristics. Plant extracts serve as a bioreductant and capping agent for the synthesis of biogenic AgNPs. Advances in the synthesis of biogenic AgNPs aim to preserve biological resources, such as replacing traditional heating methods. To achieve this, the electrolysis method is used to produce biogenic AgNPs, offering benefits such as being easy, inexpensive, fast, non-toxic, and environmentally friendly [15].

Based on the green electrosynthesis principle, a silver electrode serves as a precursor, allowing for the controlled synthesis of high-quality biogenic AgNPs with easy scaling [16]. Using a silver anode, electrosynthesis reduces the toxicity of $AgNO_3$ and the impact of metal precursor concentration on the properties of the produced AgNPs, making it preferable to bioreduction. As a result, electrosynthesis provides precise control over the form and size of AgNPs, as well as high purity, making the process more repeatable, safe, and efficient for a wide range of applications [17]. In Asian pennywort (AP), biomolecules such as alkaloids, tannins, steroids, saponins, triterpenes, and flavonoids might contribute to the synthesis of AgNPs. These biomolecules contain numerous electron-rich -OH groups [18], making them an excellent bio-medium for electrolysis. Their easily oxidisable characteristics can be used to generate AgNPs by reducing Ag^+ ions [12,19]. The AP contains triterpenes, which are anti-inflammatory compounds, as well as flavonoids, which are antioxidants [20]. Combining the electrosynthesis approach with AP biomolecules as electrolytes provides a novel study that differentiates this work from previous plant-mediated AgNP studies, especially the large-scale biosynthesis that produces biogenic AgNP with strong anti-inflammatory activity. In this work, for the first time, APE was used to electrosynthesise biogenic AgNPs, and the generated AgNPs' characteristics were investigated. The proposed AgNP-APE was evaluated for anti-inflammatory efficacy using albumin denaturation.

Materials and methods

Chemicals

The AP (Balinese accession) used in this study was obtained from near Lingsar Village, West Lombok, Indonesia. The leaves were washed under running tap water and rinsed using double-distilled water. Then, the leaves were drained at room temperature until dry and chopped. The 5 g of AP was weighed and added to 100 mL of distilled water. To prepare APE, an unmodified domestic microwave (AQUA AEM-S18125) was utilized at 80 W (20% of the total power) for 1 min, equivalent to a temperature of approximately 40 °C. The solution was then filtered and used as an electrolyte in the electrochemical synthesis of biogenic AgNPs (AgNP-APE). Silver electrode rods (Ø 1.8 mm) as precursors were purchased from Antam, Indonesia, with 99.9% purity. The phytochemical was tested using various reagents as described in the next step. Double-distilled water served as the solvent in this investigation, and all other reagents were of analytical grade.

Phytochemical test

According to a prior study, the goal of this phytochemical content test was to discover biomolecules of AP that could be involved in the synthesis of biogenic AgNP [21]. The Total Phenolic

Content (TPC) of APE was determined using the Folin-Ciocalteau reagent, with gallic acid serving as the standard. Following the addition of 1 mL of 10% Folin-Ciocalteau reagent to each 1 mL sample and 1,000 µg/mL standard, and neutralisation with 4 mL of 7.5% Na_2CO_3, the mixture was stirred for 3 h at 30 °C. The Total Flavonoid Content (TFC) of APE was determined using the $AlCl_3$ reagent, with quercetin as a reference. 10 mL of 10% $AlCl_3$ reagent was added to 1 mL of the sample and 1,000 µg/mL standard, followed by 1 mL of 1 M $C_2H_3NaO_2$, 2.8 mL of water, and an incubation period of 40 min at 30 °C. The Lieberman-Buchard reagent was used to calculate the Total Triterpene Content (TTC) of APE using ursolic acid as a standard. The quantitative analysis of triterpenes was carried out by adding 1 mL of sample and standard, 1.5 mL of chloroform, and leaving it for 3 min, then adding 100 µL of Lieberman-Buchard reagent (glacial CH_3COOH and concentrated H_2SO_4), and incubating in a dark room for 1.5 - 2 h until a precipitate formed. Then, 1.5 mL of 95% methanol was added. TFC, TPC, and TTC were determined by measuring absorbance at 415, 720, and 538 nm using a UV-visible spectrophotometer. Quantification was performed through 3 replicate measurements and a calibration curve.

Synthesis of AgNP-APE

According to Hermanto *et al.* [13,14], this electrosynthesis process uses a set of electrochemical systems consisting of a DC power source, electrodes, a polarity control switch, and a reactor. This electrolyte reactor's design was provided by earlier studies and consists of a 500 mL beaker filled with APE that rotates magnetically at 2,000 rpm at room temperature. Two silver rod electrodes immersed in APE are set 0.5 cm apart and parallel in the reactor. APE serves as an electrolyte (electron transfer medium), a bioreductant for the synthesis of biogenic AgNPs, and a stabilising/covering agent for the AgNPs. During the electrolysis process, a switch changed the polarity of the cathode and anode every minute, connecting both electrodes to a 10 V DC power supply. Once the color of the solution changed from greenish yellow to brownish yellow, biogenic AgNPs developed, and electrosynthesis was terminated. Biogenic AgNPs were collected from APE using a centrifuge (Tomy MDX-310, Japan) set to 12,000 rpm for 30 min. The pellet was separated from the remaining reactant by carefully removing the supernatant using a pipette and dried using a freeze dryer (Alpha 1-2LD plus, Germany). The pellets were then dissolved in distilled water as needed and kept in a dark bottle in the refrigerator at 5 °C until used.

Characterization of AgNP-APE

The properties of AgNP-APE obtained from the initial stage were examined using various instruments. A UV-Vis spectrophotometer (7809, Labo-Hub, China) was used to measure the localised surface plasmon resonance (LSPR) absorbance of the resulting AgNP-APE. A Fourier Transform Infra-Red (FTIR) spectrophotometer (Perkin-Elmer, USA) was used to identify the functional groups involved in the biomolecular interactions that produce AgNP-APE. To obtain microscopic images of the size distribution and shape of the resulting AgNP-APE particles, a transmission electron microscope (TEM) (Hitachi H9500, Japan) and a scanning electron microscope (JEOL-JEM, Japan) were used. In the meantime, the Debye-Scherrer equation ($D = k \lambda / \beta \cos \theta$) was used to analyse the phase morphology, crystallinity, and crystal size of AgNP-APE using X-ray diffraction (XRD) (Philips X'pert PW3050, Netherlands). where λ is the X-ray wavelength, β is the full-width at half maximum (FWHM), θ is the peak Bragg diffraction angle, D is the crystal size, and k is the form factor (0.94). The size distribution (particle size analyzer, PSA) of AgNP-APE was analyzed using a Malvern Zetasizer (Malvern Instrument, UK).

Anti-inflammatory activity of AgNP-APE

The anti-inflammatory activity of APE and AgNP-APE samples was assessed in vitro using the protein denaturation test (bovine serum albumin, BSA). The test solution (0.5 mL) contains 0.45 mL of BSA (in 5% aqueous solution) and 0.05 mL of the sample at varied concentrations (0.1 - 0.5 µg/mL). The test control solution (0.5 mL) contains 0.45 mL of BSA (in 5% aqueous solution) and 0.05 mL of control solution (saline solution) at varied concentrations (0.1 - 0.5 µg/mL). The standard solution (0.5 mL) contains 0.45 mL of BSA (in 5% aqueous solution) and 0.05 mL of standard solution at varying concentrations (0.1 - 0.5 µg/mL). Acetylsalicylic acid (aspirin 3,000 µg/mL)

served as the standard anti-inflammatory medicine. The solution was incubated for 20 min at 37 °C. After cooling, 2.5 mL of phosphate buffer (pH 6.4) was added to each solution, and the temperature was gradually increased to 70 °C over 5 min. The absorbance of the resultant solution was measured using a UV-Vis spectrophotometer at 660 nm [22]. The % inhibition of protein denaturation was calculated using the formula Eq. (1).

$$I(\%) = \frac{A_{ts} - A_{tcs}}{A_{ss}} \times 100 \quad (1)$$

Note: A_{ts} is the absorbance of the test solution, A_{tcs} is the absorbance of the product control solution, and A_{ss} is the absorbance of the standard solution. The dose-response curve was plotted, and the IC_{50} value for the sample was calculated. Each value is the result of 3 replicate measurements.

Results and discussion

Phytochemical content of APE

Biomolecules are necessary for the electrosynthesis of biogenic AgNPs utilising APE. A preliminary phytochemical analysis of APE revealed that it was proportionally high in flavonoids, phenolics, and triterpenes [5,21]. **Table 1** shows the results of the identification of the APE biomolecules employed in this study, such as TPC, TFC, and TTC. APE contains a high phenolic content, with a TPC of 122.8 ± 1.1 mg/g, in line with earlier research (**Table 1**). It has a high therapeutic and antioxidant potential due to its ability to react with active oxygen radicals via its phenolic content. APE has a significant flavonoid content, as seen by its TFC of 22.4 ± 0.7 mg/g (**Table 1**), confirming prior study findings [5]. The high concentrations of phenols and flavonoids may have a significant therapeutic influence. APE's TTC value of 6.4 ± 2.6 mg/g (**Table 1**) suggests significant triterpene levels, similar to previous investigations [5]. Triterpenes are natural chemicals found in plants that act as anti-inflammatory agents. TPC, TFC, and TTC are phytochemical components of APE that have shown therapeutic effects.

Table 1 Determination of TFC, TPC, and TTC of APE.

TPC (GAE[a] mg/g)	TFC (QE[b] mg/g)	TTC[c] (UAE mg/g)
122.8 ± 1.1	22.4 ± 0.7	6.4 ± 2.6

The Results are expressed as mg/g extract. Values are the mean ± standard deviation of triplicate analyses
[a]Gallic acid equivalence, [b]Quercetin equivalence, [c]Ursolic acid equivalence

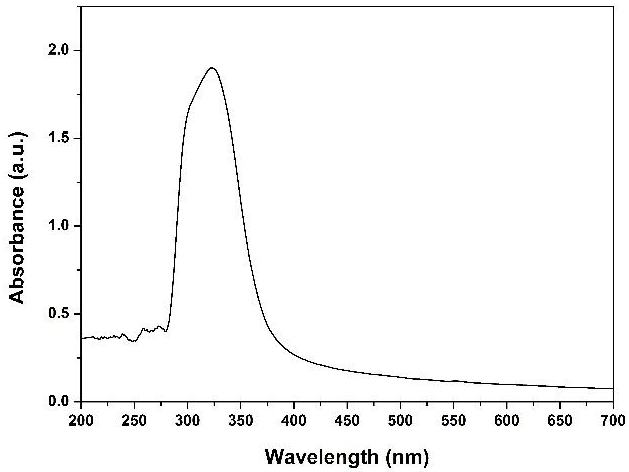

Figure 1 UV-Visible spectra of APE at with a dominant λ_{max} at 310 nm.

In addition to phytochemical content assessment, UV-Vis spectra of plant extracts (**Figure 1**) reveal the presence of numerous bioactive chemicals, including phenolic and flavonoid compounds. The interaction of

ultraviolet or visible light produces electronic transitions of bonding electrons, including sigma (σ) and pi (π) bonds, as well as non-bonding electrons (n) found in organic molecules, based on absorption peaks at certain wavelengths [23]. Carbonyl chromophores in APE (phenolics, flavonoids, and triterpenes) undergo n,π* excitation to transition from the n,π* excited state and absorb light at roughly 310 nm [24]. Several weak peaks in the 250 - 300 nm range show the π,π* excited state, which suggests the presence of biomolecules in APE with double bonds (C=C), such as triterpenes. The presence of these biomolecules is also confirmed by FTIR spectra, which will be described in the following section.

Mechanism of synthesis of AgNP-APE

A quantitative examination of the phytochemical composition of APE (**Table 1**) yielded encouraging results since it revealed the existence of biomolecules abundant in -OH (ROH) groups, such as phenols, flavonoids, and triterpenes. In addition, as reported in many previous studies, the results shown in **Figure 2(b)** indicate that there are 12 secondary metabolites of APE as reported in the prior studies [5], which are classified into 3 classes: Triterpenes (madecassoside, asiaticoside, madecassic acid, and asiatic acid), polyphenolic acids (chlorogenic acid, caffeic acid, 3,4-dicaffeoylquinic acid, 1,5-dicaffeoylquinic acid, and ellagic acid), and flavonoids (cinnaroside, scutellarin, and miquelianin). This implies that the electrosynthesis of biogenic AgNP can be carried out successfully. The production of biogenic AgNPs in an aqueous cell system with ROH-rich APE electrolyte, which serves as the electrolytic bio-media [25], is shown in **Figure 2(c)**. After dissolving, it will turn into an electrical conductor.

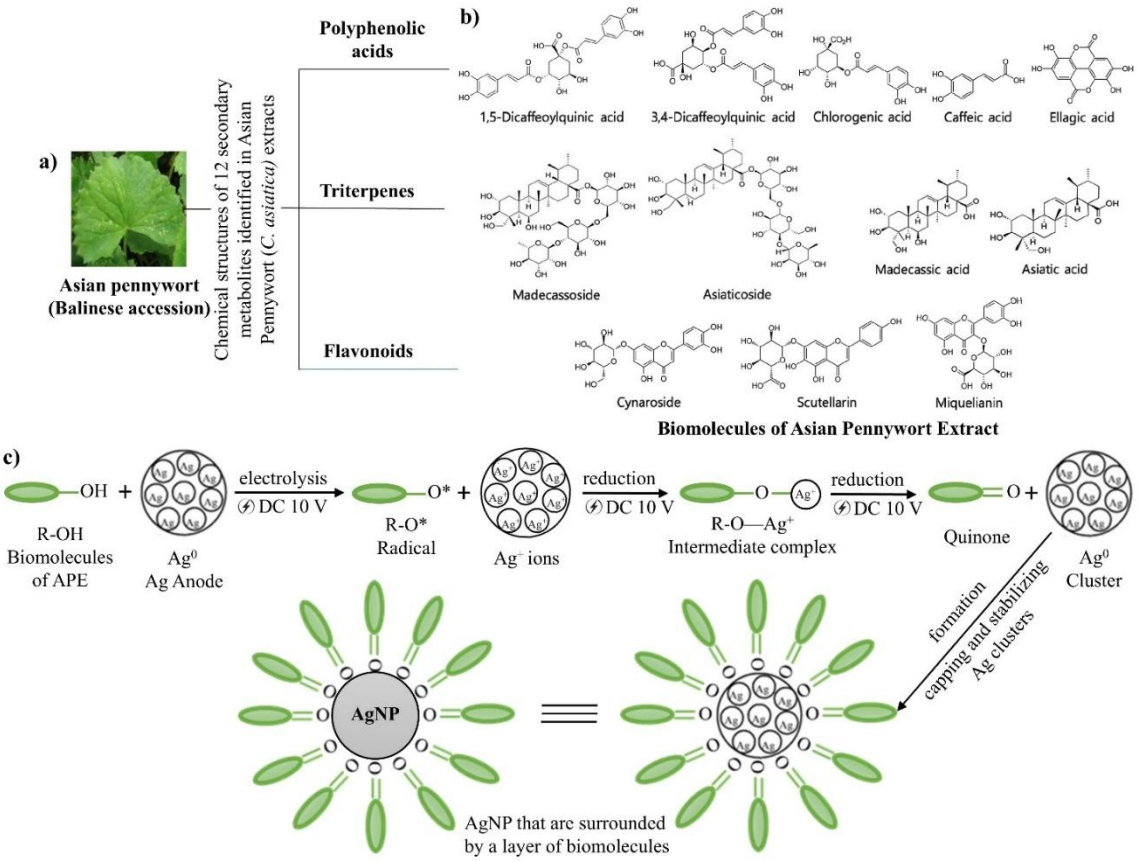

Figure 2 The AP (Balinese accession) leaves are utilised for extraction (a), the chemical structure of APE (b) [5], and the proposed mechanism of synthesis of AgNPs via electrolysis utilising APE (c).

In the first stage (**Figure 2(c)**), a DC voltage of 10 V is given to the electrolytic reactor through 2 silver rods serving as electrodes. The silver anode is oxidised to water-soluble Ag^+ ions by releasing electrons. APE

(ROH) biomolecules are transformed into RO· radicals in aqueous solution. Electrodeposition occurs at the cathode side, where Ag^+ ions travel to undergo reduction. RO radicals hinder electrodeposition on the cathode side by forming the R-O—Ag^+ intermediate complex with them [16]. In the last stage, this complex induces the formation of biogenic AgNPs. This complex allows electrostatic interactions and charge transfer between the OH groups of APE extract biomolecules and Ag^+ ions in complex, leading to bioreduction as well as the oxidation APE extract biomolecules, namely transformation of −OH groups to R=O groups (quinone) [26]. The polarity is changed every minute to prevent anode depletion caused by oxidation to Ag^+ ions. The colour of the solution changed from yellow to brownish yellow, showing that a DC voltage of 10 V facilitated the electrosynthesis of biogenic AgNP. Once a 10 V DC voltage was supplied while continuously stirring at 2,000 rpm in ambient circumstances, the intermediate complex R-O—Ag^+ was quickly produced. The R=O was formed when Ag^+ ions were reduced to Ag^0 [17]. Finally, the clustered silver particles are stabilised and coated with R=O, resulting in stable AgNPs [13,14]. It produces an AgNP template in an environment in which biomolecules surround the AgNPs and form a layer on their surface. The biomolecules surround the silver surface with physical and chemical connections, preventing particle collision and agglomeration [15,25].

APE biomolecules play an essential role in this case as bio-medium electrolytes, bioreductors, and biostabilisers of biogenic AgNP. Despite the utilisation of the same synthesis conditions (10 V voltage source), AgNPs were not produced in the electrolysis system without APE as electrolytes (water was utilised as the electrolyte medium), as in earlier research [14]. Long-term electrolysis in an aqueous medium allows for the production of water. This process combines Ag^+ ions produced by the anode and O_2 released by the cathode to form black silver oxide. Electrode deposits on the anode side cause the oxide to thicken [15]. Cheon *et al.* [27] described the electrolysis of 2 silver electrodes to produce AgNPs. After an hour of the operation, silver oxide had formed on the anode's surface. The electrolysis process stopped due to the formation of silver oxide, which interferes with the current flow. In this investigation, the anode and cathode polarities were alternated every minute to avoid water electrolysis. Thus, there are several potential advantages to the suggested biogenic AgNP electrosynthesis process, including high purity (obtained from the high-purity silver rod), facile and rapid synthesis, low cost, absence of hazardous chemicals, and simplicity in scaling up.

Characterization of AgNP-APE

Figure 3(a) shows the UV-Vis absorbance spectra of colloidal AgNP-APE with an absorption peak at 430 nm. Previous research has shown that colloidal AgNPs with particle sizes ranging from 15 to 50 nm exhibit a yellow hue and an LSPR spectrum with an absorption peak at 420 - 438 nm [13,28]. Spherical AgNPs, with a diameter of 1 - 10 nm, show an LSPR peak at a shorter wavelength. Capping and reducing agents can control the size and form of AgNPs. Solvents play an important role in the absorption of the LSPR spectrum; solvents containing biomolecule extracts are more acceptable for use, showing that the AgNPs' surface is still covered with biomolecules. The LSPR phenomenon occurs when light interacts with free electrons on the surface of nanoparticles. AgNPs absorb and scatter light at specific wavelengths, producing a specific color. This color is influenced by the size, shape, and environment surrounding the particle. In this study, the resulting AgNP solution was brownish yellow (inset of **Figure 3(a)**) with a peak at 430 nm. Based on previous research, the color and maximum wavelength indicate an AgNP size of around 15 - 50 nm, and our findings will be further confirmed by PSA and TEM data.

The functional groups of the biomolecules produced with APE that act as reducing and stabilising agents for AgNPs were determined using FTIR analysis. Furthermore, the research supported the proposed method for this product, as previously published by Loo *et al.* [19]. **Figure 3(b)** shows 6 bands identified in the right infrared spectrum: 3,434, 1,640, 1,548, 1,244, 1,086, and 400 - 800 cm^{-1}. As seen in **Figure 3(b)**, the −OH stretching mode in APE biomolecules results in an intense broad band at 3,435 cm^{-1}, which shifts from the previous band at 3,434 cm^{-1}. This is reinforced by the bending of −OH in the APE biomolecule, resulting in a band shift from 1,244 to 1,286 cm^{-1}. Biomolecules of R–OH serve as the reducing agent in the synthesis of biogenic AgNPs. The absorption peaks at 1,640 and 1,548 cm^{-1} are related to the vibration modes of the carbonyl group (C=O) and double-bonded carbon

(C=C) in the APE biomolecule. These peaks shift to 1,634 cm^{-1} and increase, indicating the presence of biomolecules that act as capping agents for AgNPs and increase their stability. A prominent intensity band shows the C=O stretching mode in quinone at 1,634 cm^{-1}. This functional group is generated from the biomolecules found in APE extract covering the surface of AgNP. The effective interaction of free electrons on C=O quinone with the unoccupied d orbital of silver [29] ensures its role as a capping agent that prevents particle aggregation via electrostatic and steric repulsion. The stretching vibration mode of the C−O group of the APE biomolecule is identified as an absorption peak at around 1,086 cm^{-1}; it experiences a peak shift to around 1,076 and 1,017 cm^{-1} indicating that the molecule plays a role in the reduction of silver ions and the presence of R-O· radicals as reaction intermediates. Finally, the FTIR spectra of electrosynthesised biogenic AgNPs reveal the formation of a weak signal in the 400 - 800 cm^{-1} region [30]. The presence of these peaks in the FT-IR spectra of electrosynthesised AgNP-APE, as shown in **Figure 3(b)**, confirms APE's dual activity as both a stabilising agent and a bioreductant [19,31].

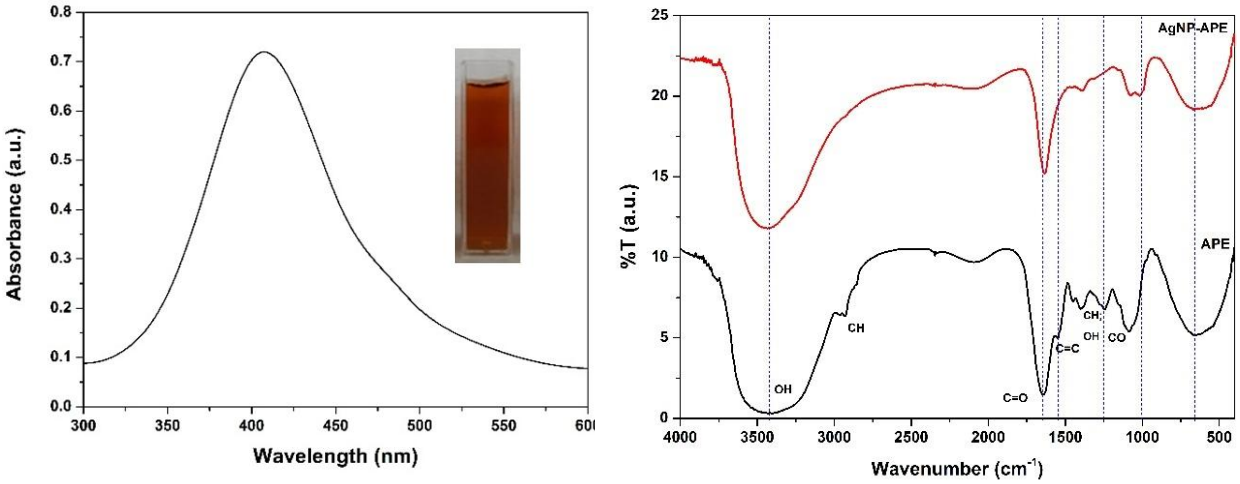

(a) (b)

Figure 3 UV-Visible absorbance spectra for AgNP-APE with LSPR at 430 nm (Inset: Photograph of AgNP-APE solutions) (a); FTIR spectra for APE— and AgNP-APE— that revealed OH, C=O, and C-O vibration shifts (b).

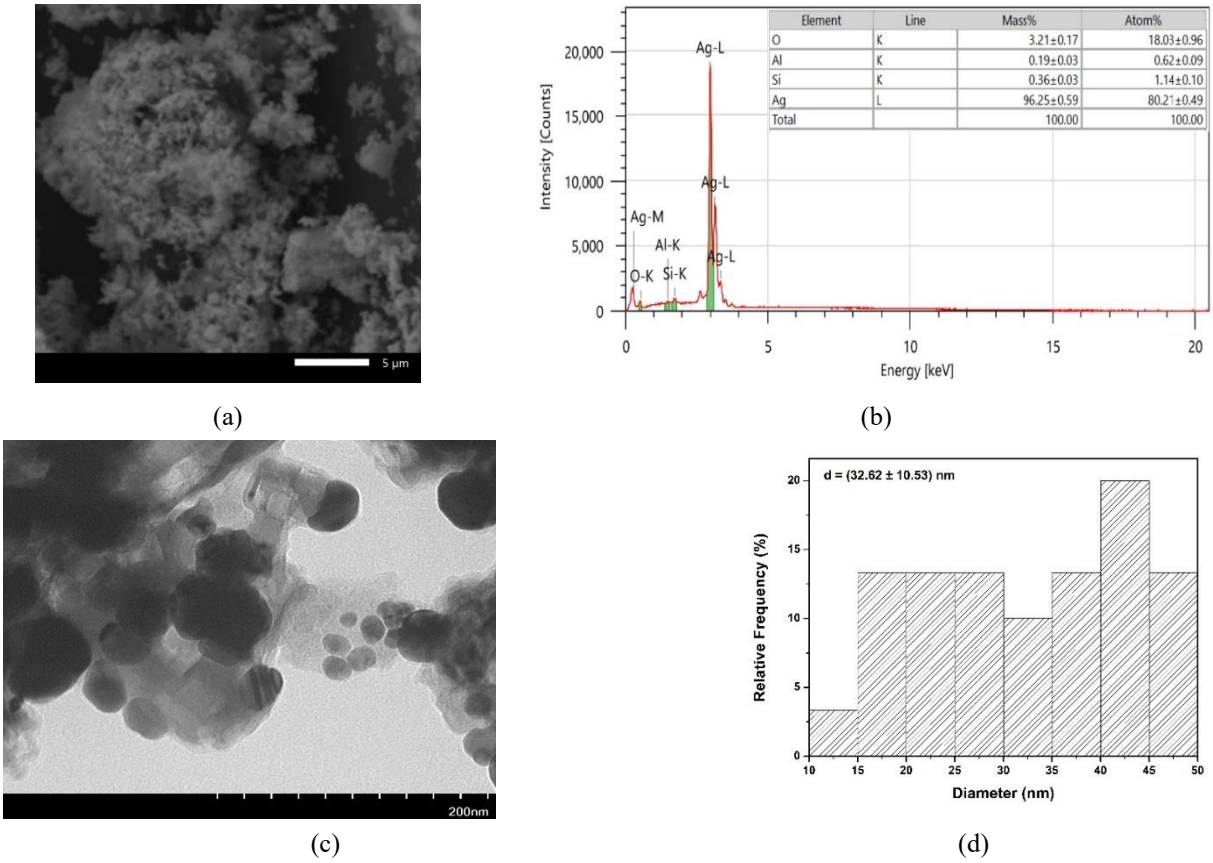

(a) (b)

(c) (d)

Figure 4 Characteristics of AgNP-APE: SEM image (a); EDS pattern (b); TEM image (c); particle size distribution (d).

SEM and TEM characterisation are electron microscopy techniques for analysing the structure and composition of nanoscale materials, whereas EDS (Energy-Dispersive X-ray Spectroscopy) characterisation is an analytical technique for identifying and measuring elements in a material. **Figure 4(a)** shows surface morphology and roughness; SEM images show that the produced AgNP-APE are mainly spherical with a rough surface. It can be attributed to complicated crystal structure, agglomeration, or uneven particle sizes. The SEM instrumentation utilised here includes EDS. The EDS pattern verifies the chemical composition of the resultant AgNP-APE, which is produced as an elemental map in **Figure 4(b)**. The ZAF method calculates the sample's weight and atomic percentage, indicating the chemical composition of the produced AgNP-APE. The silver (Ag) composition has a high purity percentage of 96.25 ± 0.59. The mass fraction of other compositions, such as O, Al, and Si, reveals the existence of APE biomolecules as coating agents and stabilisers for the produced AgNP-APE.

Using TEM examination, the size and shape of the resulting AgNP-APE were verified. In **Figure 4(c)**, it can be seen that the AgNP-APE is spherical and polydispersive, with a diameter range of 14.68 - 47.75 nm (average 32.62 nm), as shown in the size distribution histogram (Figure 4(d)). The size and shape of the resulting AgNP-APE are closely related to the variety of biomolecules in the APE extract that can cover the AgNP surface. Some of these capping agents produce electrostatic and steric repulsion, encouraging the formation of spherical AgNPs with a quite wide size range (polydispersive nanoparticles). When APE biomolecules are present, a compact interfacial layer is formed; this is related to the capacity of the biomolecules to act as coating agents. The charged surface of AgNPs and the polar oxygen groups (in this case, quinones) interact electrostatically to provide the biomolecules with coating ability [14]. The lone electron pairs of oxygen in these quinones can interact with the positive surface of AgNPs to form electrostatic interactions. AgNP-APE's FTIR spectrum further supports this interaction by showing a shift in quinone's C=O absorption from 1,640 to 1,634 cm^{-1}, which

suggests that the C=O lone electron pair is interacting with silver. Interestingly, the TEM image also shows a thin layer of other materials on the particle surface. This is likely due to a layer of extracted organic material. The organic biomolecule layer has a lower electron density than Ag, resulting in a lighter colour appearance. FTIR spectra of AgNP-APE (**Figure 3(b)**) and EDS elemental analysis (**Figure 4(b)**) and also confirmed the presence of these biomolecules. Therefore, these biomolecules act as both shape-directing and barrier agents on the AgNP surface. APE biomolecules are excellent reducing, coating, stabilising, and shaping agents, especially when nanometals are considered for biological applications.

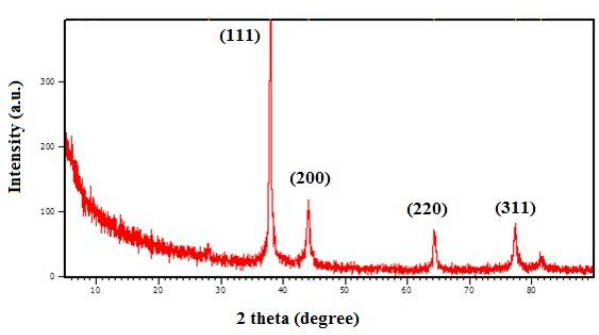

(a)

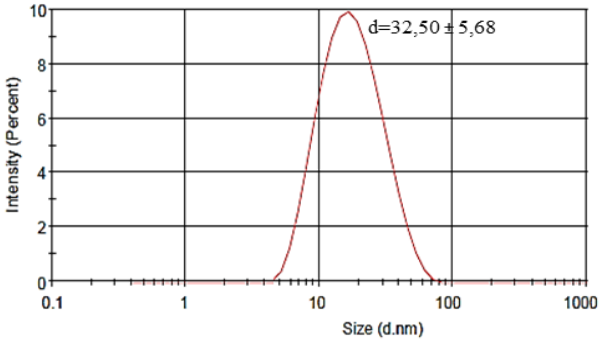

(d)

Figure 5 XRD pattern (a) and PSA profile (b) of AgNP.

Further characterisation of AgNP-APE using XRD aims to identify the phase morphology, crystallinity, and crystal size of the synthesised AgNP. Confirmation of the electrosynthetic AgNP using XRD can be seen in **Figure 4**. The XRD pattern shows a 2θ diffraction peak at 38.06°, 44.18°, 64.54°, and 77.43°, corresponding to the hkl (111), (200), (220), and (311) lattice planes, respectively, confirming the face-centred cubic (fcc) crystal structure of AgNPs (Joint Committee on Powder Diffraction Standards, JCPDS, file No. 04-0783) [32]. This finding is comparable to previous research. Additional peaks in the XRD spectrum are known to be derived from endogenous biomolecules, as well as organic and amorphous crystalline phases. These biomolecules can occasionally adsorb onto the surface of AgNPs or be integrated into their structure as in previous research [33]. This is also confirmed by FTIR, EDS, and TEM data of AgNP-APE. The Debye-Scherrer equation was used to calculate the size of the Ag crystals produced, which ranged between 17.55 and 32.26 nm.

Nanoparticle characterisation with PSA is a method to measure particle size distribution in a sample. The particle size distribution of AgNP-APE was evaluated in a colloidal environment and verified by PSA. The size distribution of AgNP-APE was approximately 32.50 nm, based on the PSA profile (**Figure 5(a)**). The design, manufacturing, and manipulation of particle architectures with sizes ranging from 1 to 100 nm are the focus of nanotechnology approaches, and the resulting biogenic AgNPs remained within this range. The agreement of the UV-Vis spectra (**Figure 3(a)**), particle size histogram (**Figure 4(d)**), and PSA profile (**Figure 5(a)**) confirmed that the size of the obtained AgNP-APE was approximately 32 nm. The small size of AgNP-APE gives them a high surface-area-to-volume ratio. Smaller particles have more exposed surface area relative to the amount of material they contain, increasing the surface area-to-volume ratio. This allows more silver atoms on the surface to come into contact with the surrounding environment, which contributes to their unique physical and chemical properties, including their therapeutic activity.

Anti-Inflammatory Activity of AgNP-APE

Bovine Serum Albumin (BSA) protein is utilised in anti-inflammatory activity assays as a model protein that denatures (changes in form and function). Heat-induced protein denaturation serves as an indicator of a compound's anti-inflammatory efficacy. The standard temperature is 37 °C, which is gradually increased to 70 °C over time. The ability to stabilise protein or prevent BSA denaturation indicates that a substance has anti-inflammatory properties [22]. The IC_{50} value represents

the level of anti-inflammatory activity. The stronger the anti-inflammatory qualities in preventing the inflammatory process, the lower the IC_{50} number. The IC_{50} value represents the concentration of the substance necessary to inhibit a biological activity, such as inflammation, by 50%; lower values indicate more efficacy in inhibition or reducing protein denaturation. **Figure 6** shows the anti-inflammatory activity test of APE, AgNP-APE, and acetylsalicylic acid (as a reference) for *in vitro* inhibition of protein denaturation testing of BSA.

Based on **Figure 6(a)**, the anti-inflammatory activity of APE, AgNP-APE, and the reference drug shows an incremental pattern as the concentration increases, with a high inhibition percentage at 1,000 µg/mL. The activity increases with increasing dose. Furthermore, the magnitude is expressed as IC_{50} (calculated from the linear equation of the dose-response curve, **Figure 6(b)** APE at various concentrations shows a not too high anti-inflammatory potential (7-47%) with an IC_{50} of 960.29 ±16.81 µg/mL against BSA denaturation, while AgNP-APE at various concentrations shows a fairly high anti-inflammatory potential (13% - 89%) with an IC_{50} of 523.40 ± 7.85 µg/mL against BSA denaturation, with both being compared to synthetic drugs (aspirin) (having an IC_{50} of 355.57 ± 5.69 µg/mL). Due to the lowest IC_{50} value, aspirin as a standard had the strongest anti-inflammatory activity, followed by AgNP-APE and APE, respectively. The AgNP-APE produced could enhance the APE's anti-inflammatory activity.

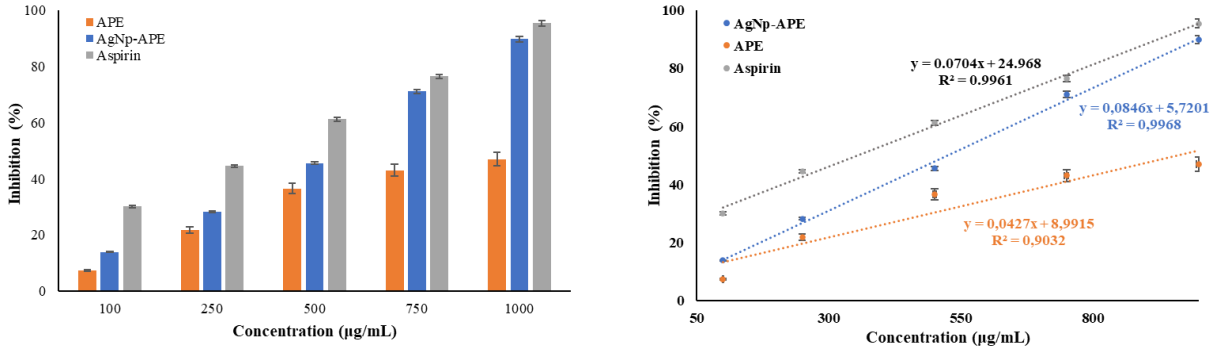

(a) (b)

Figure 6 The BSA anti-inflammatory activity of the APE, AgNP-APE, and the reference drug (aspirin) is showing an inhibition pattern (a) and a dose-response curve (b).

APE is known to have strong anti-inflammatory properties, thanks to bioactive compounds such as triterpenes (asiaticoside, madecassoside, asiatic acid, and madecassic acid) that play a role in reducing inflammation [34]. Biogenic AgNP-APE shows stronger anti-inflammatory properties than APE. The role of metal nanoparticles coated with APE biomolecules enhances their anti-inflammatory properties. The BSA protein denaturation test is used to assess the ability of a compound to prevent or inhibit this denaturation process, which is an indication of anti-inflammatory properties [35]. The interaction of AgNP with proteins involves several complex molecular mechanisms. AgNPs can interact directly with proteins through various bonds, such as electrostatic bonds, disulfide bonds, hydrogen bonds, or hydrophobic interactions. These interactions can stabilise the protein structure and prevent it from conformational changes that cause denaturation. AgNP can act as a shield or barrier between proteins and denaturing agents, such as heat, chemicals, or enzymes. Thus, AgNP can reduce the impact of denaturing agents on proteins, thereby preventing or slowing the denaturation process. Protein denaturation is often associated with oxidative stress. AgNPs are known to act as antioxidants, meaning they can reduce oxidative stress in cells or solutions. By reducing oxidative stress, AgNPs can help prevent or slow down protein denaturation caused by oxidative stress. Furthermore, AgNPs can induce conformational changes in certain proteins. Through electrostatic

interactions, proteins and the AgNP surface can interact, leading to protein adsorption and structural changes in the protein's 3 dimensions. This conformational alteration may significantly change the protein's functional properties, as well as the overall biological activity of AgNPs [36]. These changes can be stable and help the protein maintain its structure, or they can be transient and help the protein adapt to environmental conditions. It should be noted that the mechanism of action of AgNPs in inhibiting protein denaturation can vary depending on the type of protein, environmental conditions, and the properties of the AgNPs themselves (size, shape, surface charge, etc.) [37].

Synthetic NSAIDs have significant drawbacks and side effects for inflammation [1]. Common side effects include nausea, heartburn, and indigestion; dizziness or drowsiness; and ringing in the ears. Natural products are gaining popularity over traditional medicines due to their accessibility, consistency, cost-effectiveness, reduced risk of toxicity and side effects, increased safety, and effectiveness. Analgesic, anti-inflammatory, and anti-arthritis drugs can be developed using plant-derived phytochemicals that can inhibit the denaturation of protein inhibitors [38]. Thus, our study demonstrates that APE can suppress and prevent protein denaturation. Enhanced anti-inflammatory efficacy is achieved by embedding AgNPs within APE biomolecules. AgNP-APE is easy to prepare, inexpensive, non-toxic, and has potential as an anti-inflammatory agent. Thus, this study encourages the development of promising plant-based AgNPs as anti-inflammatory agents on a large scale compared to other green synthesis routes.

Conclusions

The green electrosynthesis approach, utilising APE, was used to synthesise AgNPs in an environmentally benign and sustainable manner. Biomolecules in the APE serve as a bio-media, bioreductor, capping, and stabilising agent throughout the AgNP production process. The APE's phytochemical screening revealed the phenols, flavonoids, and triterpenes. The produced AgNPs have a face-centred cubic (fcc) crystal structure and uniform spherical shape, surrounded by a thin biomolecular layer. Its diameters range from 32 nm. APE and synthesised AgNPs exhibit high in vitro anti-inflammatory activity, Electrosynthesis of biogenic AgNPs improves APE's anti-inflammatory activity, lowering the IC_{50} from 960.29 ±16.81 to 523.40 ± 7.85 µg/mL of AgNP-APE. With its superior features and activity, a large-scale biosynthesis approaches combining electrosynthesis with biomolecular APE offers promising future applicability, particularly in the pharmaceutical and cosmetics industries.

Acknowledgements

The authors thank the Ministry of Education, Culture, Research, and Technology, Republic of Indonesia, through grant Penelitian Fundamental Reguler, PFR (contract number: 4394/UN18.L1/PP/2025).

Declaration of Generative AI in Scientific Writing

I have not utilised artificial intelligence (AI) tools, including language models, to create, write, or alter any portion of this paper.

CRediT Author Statement

Dhony Hermanto: Conceptualization; Methodology; Writing - Original draft; Supervision. **Nurul Ismillayli:** Validation; Formal analysis; Investigation. **Rahadi Wirawan:** Data curation; Visualization; Software. All authors: Writing - Reviewing & Editing.

References

[1] E Auriel, K Regev and AD Korczyn. *Nonsteroidal anti-inflammatory drugs exposure and the central nervous system*. *In*: A Quartarone, MF Ghilardi and F Boller (Eds.). Handbook of clinical neurology. Elsevier, Amsterdam, Netherlands, 2014, p. 577-584.

[2] FWD Tai and ME McAlindon. Non-steroidal anti-inflammatory drugs and the gastrointestinal tract. *Clinical Medicine, Journal of the Royal College of Physicians of London* 2021; **21(2)**, 131-134.

[3] ZS Ololade, SE Kuyooro, OO Ogunmola and OO Abiona. Phytochemical, antioxidant, anti-arthritic, anti-inflammatory and bactericidal potentials of the leaf extract of lactuca teraxacifolia. *Global Journal of Medical Research B: Pharma, Drug Discovery* 2017; **17(2)**, 19-28.

[4] M Qureshi, N Jahan, S Muhammad, N Mohani, A Wazir, IA Baig and M Ahmad. Evaluation of

neuropharmacological, analgesic and anti-inflammatory effects of the extract of *Centella asiatica* (Gotu kola) in mice. *African Journal of Pharmacy and Pharmacology* 2015; **9(41)**, 995-1001.

[5] HY Shin, H Kim, S Jung, EJ Jeong, KH Lee, YJ Bae, HJ Suh, KI Jang and KW Yu. Interrelationship between secondary metabolites and antioxidant capacities of Centella asiatica using bivariate and multivariate correlation analyses. *Applied Biological Chemistry* 2021; **64(82)**, 1-10.

[6] I Ahmad, MN Khan, K Hayat, T Ahmad, DF Shams, W Khan, V Tirth, G Rehman, W Muhammad, MElhadi, A. Alotaibi and SK Shah. Investigating the antibacterial and anti-inflammatory potential of polyol-synthesized silver nanoparticles. *ACS Omega* 2023; **9(11)**, 13208-13216.

[7] NTL Chi, M Narayanan, A Chinnathambi, C Govindasamy, B Subramani, K Brindhadevi, T Pimpimon and S Pikulkaew. Fabrication, characterization, anti-inflammatory, and anti-diabetic activity of silver nanoparticles synthesized from Azadirachta indica kernel aqueous extract. *Environmental Research* 2022; **208**, 112684.

[8] RM Varghese, A Kumar and R Shanmugam. Comparative Anti-inflammatory activity of silver and zinc oxide nanoparticles synthesized using *Ocimum tenuiflorum* and *Ocimum gratissimum* herbal formulations. *Cureus* 2024; **16(1)**, e52995.

[9] N Ismillayli, S Suprapto, E Santoso, RE Nugraha, H Holilah, H Bahruji, AA Jalil, D Hermanto and D Prasetyoko. The role of pH-induced tautomerism of polyvinylpyrrolidone on the size, stability, and antioxidant and antibacterial activities of silver nanoparticles synthesized using microwave radiation. *RSC Advance* 2024; **14(7)**, 4509-4517.

[10] I Fatimah, H Hidayat, BH Nugroho and S Husein. Ultrasound-assisted biosynthesis of silver and gold nanoparticles using Clitoria ternatea flower. *South African Journal of Chemical Engineering* 2020; **34**, 97-106.

[11] S Kaabipour and S Hemmati. A review on the green and sustainable synthesis of silver nanoparticles and one-dimensional silver nanostructures. *Beilstein Journal of Nanotechnology* 2021; **12**, 102-136.

[12] Q Sun, X Cai, J Li, M Zheng, Z Chen and CP Yu. Green synthesis of silver nanoparticles using tea leaf extract and evaluation of their stability and antibacterial activity. *Colloids and Surfaces A: Physicochemical and Engineering Aspects* 2014; **444**, 226-231.

[13] D Hermanto, N Ismillayli, I Irmawanti, I Fathulloh, D Nila, UK Zuryati, H Muliasari and R Wirawan. Electrochemically synthesized biogenic silver nanoparticles using green tea extract as a promising antioxidant. *Karbala International Journal of Modern Science* 2023; **9(1)**, 80-88.

[14] D Hermanto, N Ismillayli, DH Fatwa, UK Zuryati, H Muliasari, R Wirawan, D Prasetyoko and S Suprapto. Bio-mediated electrochemically synthesis of silver nanoparticles using green tea (Camellia sinensis) leaves extract and their antibacterial activity. *South African Journal of Chemical Engineering* 2024; **47(1)**, 136-141.

[15] E Daun, BK Siswanta, S Siswoyo, S Suprapto and D Prasetyoko. Electrosynthesis of anisotropic biogenic silver nanoparticles as a promising antibacterial agent using *Stachytarpheta jamaicensis* leaf extract. *Sains Malaysiana* 2024; **53(9)**, 3113-3123.

[16] Z Huang, H Jiang, P Liu, J Sun, D Guo, J Shan and N Gu. Continuous synthesis of size-tunable silver nanoparticles by a green electrolysis method and multi-electrode design for high yield. *Journal of Materials Chemistry A* 2015; **3(5)**, 1925-1929.

[17] VT Hoang, NX Dinh, TN Pham, TV Hoang, PA Tuan, TQ Huy and AT Le. Scalable electrochemical synthesis of novel biogenic silver nanoparticles and its application to high-sensitive detection of 4-nitrophenol in an aqueous system. *Advances in Polymer Technology* 2021; **2021**, 664219.

[18] C Tsou and R Yang. *Low cost green synthesis of silver nanoparticles using taiwan oolong tea extract. In*: RJ Yang (Ed.). Importance & applications of nanotechnology. MedDocs, Nevada, United States, 2020, p. 1-5.

[19] YY Loo, BW Chieng, M Nishibuchi and S Radu. Synthesis of silver nanoparticles by using tea leaf

extract from *Camellia Sinensis*. *International Journal of Nanomedicine* 2012; **7**, 4263-4267.

[20] BN Ramesh, TK Girish, RH Raghavendra, KA Naidu, UJSP Rao and KS Rao. Comparative study on anti-oxidant and anti-inflammatory activities of *Caesalpinia crista* and *Centella asiatica* leaf extracts. *Journal of Pharmacy and Bioallied Sciences* 2014; **6(2)**, 86-91.

[21] A Kandasamy, K Aruchamy, P Rangasamy, D Varadhaiyan, C Gowri, TH Oh, S Ramasundaram and B Athinarayanan. Phytochemical analysis and antioxidant activity of *Centella asiatica* extracts: An experimental and theoretical investigation of flavonoids. *Plants* 2023; **12(20)**, 13547.

[22] P Salve, A Vinchurkar, R Raut, R Chondekar, J Lakkakula, A Roy, MJ Hossain, S Alghamdi, MAlmehmadi, O Abdulaziz, M Allahyani, AS Dablool, MR Sarker and MFN Azlina. An evaluation of antimicrobial, anticancer, anti-inflammatory, and antioxidant activities of silver nanoparticles synthesized from leaf extract of *Madhuca longifolia* utilizing quantitative and qualitative methods. *Molecules* 2022; **27(19)**, 6404.

[23] RA Pratiwi and ABD Nandiyanto. How to read and interpret uv-vis spectrophotometric results in determining the structure of chemical compounds. *Indonesian Journal of Educational Research and Technology* 2022; **2(1)**, 1-20.

[24] TK Patle, K Shrivas, R Kurrey, S Upadhyay, R Jangde and R Chauhan. Phytochemical screening and determination of phenolics and flavonoids in Dillenia pentagyna using UV-Vis and FTIR spectroscopy. *Spectrochimica Acta - Part A: Molecular and Biomolecular Spectroscopy* 2020; **242**, 118717.

[25] VV Yanilkin, RR Fazleeva, GR Nasretdinova, NV Nastapova and YN Osin. Methylviologen-mediated electrosynthesis of silver nanoparticles in a water medium. Effect of chain length and concentration of poly(n-vinylpyrrolidone) on particle size. *New Materials, Compounds and Applications* 2018; **2(1)**, 28-41.

[26] WA Shaikh, S Chakraborty, G Owens and RU Islam. A review of the phytochemical mediated synthesis of AgNP (silver nanoparticle): the wonder particle of the past decade. *Applied Nanoscience* 2021; **11**, 2625-2660.

[27] JM Cheon, JH Lee, Y Song and J Kim. Synthesis of Ag nanoparticles using an electrolysis method and application to inkjet printing. *Colloids and Surfaces A: Physicochemical and Engineering Aspects* 2011; **389(1-3)**, 175-179.

[28] R Roto, M Marcelina, NH Aprilita, M Mudasir, TA Natsir and B Mellisani. Investigation on the effect of the addition of Fe^{3+} ion into the colloidal AgNPs in PVA solution and understanding its reaction mechanism. *Indonesian Journal of Chemistry* 2017; **17(3)**, 439-445.

[29] S Muthaiah, A Bhatia and M Kannan. *Stability of metal complexes*. *In*: AN Srivastva (Ed.). Stability and applications of coordination compounds. Intechopen, London, 2020, p. 1-18.

[30] IIK Siakavella, F Lamari, D Papoulis, M Orkoula, P Gkolfi, M Lykouras, K Avgoustakis and S Hatziantoniou. Effect of plant extracts on the characteristics of silver nanoparticles for topical application. *Pharmaceutics* 2020; **12(12)**, 1244.

[31] A Wirwis and Z Sadowski. Green synthesis of silver nanoparticles: Optimizing green tea leaf extraction for enhanced physicochemical properties. *ACS Omega* 2023; **8(33)**, 30532-30549.

[32] N Agasti and NK Kaushik. One-pot synthesis of crystalline silver nanoparticles. *American Journal of Nanomaterials* 2014; **2(1)**, 4-7.

[33] SE Arland and J Kumar. Green and chemical syntheses of silver nanoparticles: Comparative and comprehensive study on characterization, therapeutic potential, and cytotoxicity. *European Journal of Medicinal Chemistry Reports* 2024; **11**, 100168.

[34] K Ali, S Kumar and MF Khan. A concise review on bioactive pentacyclic triterpenoids of *Centella asiatica* (Gotu Kola). *Discover Chemistry* 2025; **2(1)**, 1-21.

[35] JM Carvalho-Silva and ACD Reis. Anti-inflammatory action of silver nanoparticles in vivo: systematic review and meta-analysis. *Heliyon* 2024; **10(14)**, 34564.

[36] CN Roy, S Maiti, TK Das, S Kundu, S Karmakar and A Saha. Investigation on silver nanocrystals induced structural modulation of biomarker alkaline phosphatase through spectroscopic and

thermodynamic assessment. *Journal of Molecular Structure* 2024; **1315**, 138792.

[37] MS Akhter, A Rahman, RK Ripon, M Mubarak, M Akter, S Mahbub, FA Mamun and T Sikder. A systematic review on green synthesis of silver nanoparticles using plants extract and their bio-medical applications. *Heliyon* 2024; **10**, 29766.

[38] YH Gonfa, FB Tessema, A Bachheti, N Rai, MG Tadesse, AN Singab, KK Chaubey and RK Bachheti. Anti-inflammatory activity of phytochemicals from medicinal plants and their nanoparticles: A review. *Current Research in Biotechnology* 2023; **6**, 100152.